



This is a repository copy of *Boundary admittance estimation for wave-based acoustic simulations using Bayesian inference*.

White Rose Research Online URL for this paper:

<https://eprints.whiterose.ac.uk/193009/>

Version: Published Version

Article:

Chen, Z., Xiang, N. and Horoshenkov, K.V. orcid.org/0000-0002-6188-0369 (2022)
Boundary admittance estimation for wave-based acoustic simulations using Bayesian inference. *JASA Express Letters*, 2 (8). 081601. ISSN 2691-1191

<https://doi.org/10.1121/10.0012992>

Reuse

This article is distributed under the terms of the Creative Commons Attribution (CC BY) licence. This licence allows you to distribute, remix, tweak, and build upon the work, even commercially, as long as you credit the authors for the original work. More information and the full terms of the licence here:

<https://creativecommons.org/licenses/>

Takedown

If you consider content in White Rose Research Online to be in breach of UK law, please notify us by emailing eprints@whiterose.ac.uk including the URL of the record and the reason for the withdrawal request.



eprints@whiterose.ac.uk
<https://eprints.whiterose.ac.uk/>

Boundary admittance estimation for wave-based acoustic simulations using Bayesian inference

Ziqi Chen,¹ Ning Xiang,^{1,a)} and Kirill V. Horoshenkov²

¹Graduate Program in Architectural Acoustics, School of Architecture, Rensselaer Polytechnic Institute, Troy, New York 12180, USA

²Department of Mechanical Engineering, University of Sheffield, Sheffield, United Kingdom
chenz33@rpi.edu, xiangn@rpi.edu, k.horoshenkov@sheffield.ac.uk

Abstract: Acoustic surface admittance/impedance at domain boundaries is essential for wave-based acoustic simulations. This work applies two levels of Bayesian inference to estimate the order and the parameter values of the multipole admittance model. The frequency-dependent acoustic admittance is experimentally measured. Incorporating the maximum entropy strategy, the unified Bayesian framework is applied to the multipole approximation. Analysis results demonstrate that multipole model-based Bayesian inference is well suited to estimating the arbitrary frequency-dependent boundary condition within a wave-based simulation framework. © 2022 Author(s). All article content, except where otherwise noted, is licensed under a Creative Commons Attribution (CC BY) license (<http://creativecommons.org/licenses/by/4.0/>).

[Editor: Shiu Keung Tang]

<https://doi.org/10.1121/10.0012992>

Received: 31 January 2022 **Accepted:** 26 June 2022 **Published Online:** 1 August 2022

1. Introduction

In room acoustics, simulations play an important role in exploring sound propagation in an enclosed space, useful in many fields, like building and vehicle design. Boundary conditions are essential for wave-based acoustic simulations. This paper proposes a method to generate the frequency-dependent surface impedance/admittance through a model-based probabilistic approach. The boundary estimation and simulation have drawn much attention (Bin *et al.*, 2009; Pind *et al.*, 2020). de l'Épine *et al.* (2005) applied a Bayesian identification approach to estimating surface impedance of duct liners under air flows, but few works have dealt with the selection of a concise model order that is computationally more efficient than any overfit models. This work focuses on the concise model of boundary admittance given the surface impedance/admittance as a function of frequency. This paper demonstrates that Bayesian inference can estimate the order of models and the parameters in each model (Xiang, 2020) given the experimentally measured boundary impedance. The multipole model can be estimated from the surface impedance/admittance out of the measurement frequency range.

This paper is organized as follows. Section 2 introduces a parametric model used for Bayesian inference. Section 3 discusses the concept of two levels of the inference, and Sec. 4 explains the principle of maximum entropy for the prior probability assignment. Section 5 discusses the implementation of the nested sampling. Section 6 presents the experimental results. Section 7 concludes the paper.

2. Wave-based multipole model

The boundary conditions play an important role in wave-based room-acoustic simulations. Many models have been proposed to describe the complex boundary conditions. Fung and Ju (2001) introduces a broadband model for reflection coefficients. Reyman *et al.* (2008) and Dagna *et al.* (2015) implemented a multipole broadband impedance model in the recursive convolution, and Pind *et al.* (2019) implemented this model for the spectral element method. Rienstra (2006) introduced an extended Helmholtz resonator model. Horoshenkov *et al.* (2019) proposed a Padé approximation model to predict the acoustical properties of porous materials. However, the choice of model orders has not been fully discussed in this work. Dagna *et al.* (2015) used the vector fitting method to obtain the coefficient parameters and compare the performance of the multipole models through approximation error, yet no effort was undertaken to select an appropriate order of the model. The multipole approximation of surface impedance/admittance is mostly used in time-domain approaches. Indeed, the translation of the surface impedance/admittance boundary condition into the time-domain in a convolution requires massive computation. The multipole approximation provides an efficient method to evaluate the convolution.

The complex-valued surface admittance in the frequency domain $\underline{G}_s(\omega)$ is determined as

^{a)} Author to whom correspondence should be addressed.

$$\underline{G}_s(\omega) = \frac{\underline{V}(\omega)}{\underline{P}(\omega)} = \frac{1}{\underline{Z}_s(\omega)}, \tag{1}$$

where $\underline{P}(\omega)$ is the sound pressure spectrum at the boundary surface in the frequency domain, $\underline{V}(\omega)$ is the particle velocity spectrum normal to the surface in the frequency domain, $\underline{Z}_s(\omega)$ is the frequency-dependent surface impedance, and ω is the angular frequency. In this work, a so-called multipole broadband impedance model is used to describe the frequency-dependent admittance (Troian *et al.*, 2017) as follows:

$$\underline{G}_s(\omega) = G_\infty + \sum_{q=1}^Q \frac{A_q}{\lambda_q + j\omega} + \sum_{s=1}^S \left(\frac{\underline{\Theta}_s}{\underline{\theta}_s + j\omega} + \frac{\underline{\Theta}_s^*}{\underline{\theta}_s^* + j\omega} \right), \tag{2}$$

with

$$\underline{\Theta}_s = B_s + jC_s, \quad \underline{\theta}_s = \alpha_s + j\beta_s, \tag{3}$$

where Q is the number of real-valued poles, λ_q , S is the number of complex-values pole pairs, $[\theta_s, \theta_s^*]$. G_∞ is the high-frequency limit of the admittance $\underline{G}_s(\omega)$, and A_q , B_s , and C_s are real-valued coefficients. A model with $Q=x$ and $S=y$ means that this model has x real-valued poles and y pairs of complex-values poles. For convenience, a model with $Q=x$ and $S=y$ is referred to as a $QxSy$ model in the rest of this paper. Two main advantages come with this multipole model: small computational cost for the simulation and easy solution to the causality problem. To ensure the system is causal and real, the parameters need to satisfy the constraint $\{A_q, B_s, C_s, \beta_s\} \in \mathbb{R}$ and $\{\lambda_q, \alpha_s\} \in \mathbb{R}^+$ (Dragna *et al.*, 2015). In the wave-based room-acoustic simulation, a more complex boundary model requires more memory buffers and computation steps in the numerical implementation on the boundaries. Take the finite-difference time-domain method as an example. When Q increases to $x_0 + 1$ from x_0 , one more buffer is needed for the entire boundaries. At the same time, two more buffers are required for the simulation when this increase happens to S .

3. Bayesian inference

This work focuses first on a parsimonious order and then estimates the model parameters given that order. The multipole admittance models of different numbers of poles in Eq. (2) are applied to fit the experimental data obtained for acoustic measurements, which are complex-valued admittance as a function of frequency, denoted in the following as \mathbf{D} . The surface admittance estimation involves two levels of Bayesian inference. This work estimates the order Q and S of the multipole admittance model through the higher level of inference, Bayesian model selection. The first (lower) level of inference, Bayesian parameter estimation, is applied to estimate the parameter values of the surface admittance model once the model order is selected.

3.1 Model selection

Given a finite set of models of different orders that are competing against each other to explain the data, the model that fits the data best is not always the best choice for room-acoustic simulations. An increase in model complexity tends to result in a better match between the experimental data and the models but is likely to cause overfit, which is a phenomenon in which the models fit everything including noise and predict nothing accurately. To penalize overfit, Bayesian model selection applies Bayes's theorem to one model \mathbf{H}_i among a finite set of models $\mathbf{H}_1, \mathbf{H}_2, \dots, \mathbf{H}_M$, given the experimental data \mathbf{D} and the background information I that *the model is able to describe the data well*. In this case, Bayes's theorem can be written as

$$p(\mathbf{H}_i|\mathbf{D}, I) = \frac{p(\mathbf{D}|\mathbf{H}_i, I)p(\mathbf{H}_i|I)}{p(\mathbf{D}|I)}, \tag{4}$$

where $p(\mathbf{H}_i|\mathbf{D}, I)$ is the posterior probability of the model \mathbf{H}_i , $p(\mathbf{H}_i|I)$ is the prior probability of the model \mathbf{H}_i , and $p(\mathbf{D}|\mathbf{H}_i, I)$ is the marginal likelihood of the model \mathbf{H}_i given the experimental data \mathbf{D} , which is also referred to as Bayesian evidence. Note that the models competing against each other in this work are the models described in Eq. (2) with different Q and S .

For the purpose of evaluating the models, the Bayes factor (Kass and Raftery, 1995; Xiang, 2020) is calculated to enable the quantitative comparison between model \mathbf{H}_i and \mathbf{H}_j as

$$B_{ij} = \frac{p(\mathbf{H}_i|\mathbf{D}, I)}{p(\mathbf{H}_j|\mathbf{D}, I)} = \frac{p(\mathbf{D}|\mathbf{H}_i, I)}{p(\mathbf{D}|\mathbf{H}_j, I)}, \quad i \neq j, \tag{5}$$

with no preference to any of the models—the prior probabilities of models are uniform (Xiang, 2020). The Bayes factor is often evaluated in a logarithmic scale,

$$L_{ij} = 10 \log_{10}(B_{ij}) = 10 \log_{10}(Z_i) - 10 \log_{10}(Z_j) \quad [\text{deciban}], \tag{6}$$

where $Z_i = p(\mathbf{D}|\mathbf{H}_i, I)$ is a simplified notation for the Bayesian evidence of model \mathbf{H}_i . The highest positive value of Bayes factors indicates that model \mathbf{H}_i is preferred by the data over the model \mathbf{H}_j the most.

3.2 Parameter estimation

Once a multipole model is selected in Sec. 3.1, the Bayesian theorem is applied to estimate its parameters ϑ encapsulated inside the selected model, denoted as $\mathbf{H}(\vartheta)$. To be more precise, the broadband admittance model contains a specific set of parameters, which is collectively denoted as ϑ , including the offset G_{∞} , the poles, and their coefficients, given the experimental data \mathbf{D} and the background information I . The parameter estimation applying the Bayesian theorem yields

$$p(\vartheta|\mathbf{H}, \mathbf{D}, I) = \frac{p(\mathbf{D}|\vartheta, \mathbf{H}, I)p(\vartheta|\mathbf{H}, I)}{p(\mathbf{D}|\mathbf{H}, I)}, \tag{7}$$

where probability $p(\vartheta|\mathbf{H}, \mathbf{D}, I)$ is known as the posterior probability distribution of parameters ϑ . $p(\mathbf{D}|\vartheta, \mathbf{H}, I)$ is the likelihood function that the experimental data \mathbf{D} would be generated given the parameter set ϑ and the model \mathbf{H} . $p(\vartheta|\mathbf{H}, I)$ represents the prior probability of the parameters given the model \mathbf{H} . The denominator $p(\mathbf{D}|\mathbf{H}, I)$ is known as (Bayesian) evidence. Note that the evidence $p(\mathbf{D}|\mathbf{H}, I)$ is the same as the marginal likelihood in Eqs. (4) and (5). Equation (7) expresses how the prior knowledge of the parameters is updated in the presence of the data through the likelihood.

3.3 Unified framework

The integration of a proper probability density over the entire parameter space must be equal to unity (Xiang, 2020). Thus, integrating both sides of Eq. (7) leads to

$$Z = p(\mathbf{D}|\mathbf{H}, I) = \int_{\vartheta} p(\mathbf{D}|\vartheta, \mathbf{H}, I)p(\vartheta|\mathbf{H}, I)d\vartheta. \tag{8}$$

This equation indicates that Bayesian evidence is calculated by integrating the product of the likelihood and prior probability over the entire parameter space. Since this is the same evidence as in Eqs. (4) and (5), both levels of inference can be unified. The shorthand notations $\Pi(\vartheta) = p(\vartheta|\mathbf{H}, I)$, $Z = p(\mathbf{D}|\mathbf{H}, I)$, as in Eq. (8), are used for simplification, and Eq. (4) can be rewritten as

$$\underbrace{p(\vartheta|\mathbf{D}, \mathbf{H}, I)}_{\text{posterior}} \cdot \underbrace{Z}_{\text{evidence}} = \underbrace{p(\mathbf{D}|\vartheta, \mathbf{H}, I)}_{\text{likelihood}} \cdot \underbrace{\Pi(\vartheta)}_{\text{prior}}. \tag{9}$$

The left-hand side of Eq. (9) contains outputs of the inference, while the right-hand side contains two inputs. These inputs are two prior probabilities. Equation (8) implies the evaluation of the Bayesian evidence requires the full exploration of the likelihood over the entire parameter space. Equations (8) and (9) indicate that the evidence is important for the model selection, while the posterior plays a central role in the parameter estimation. Equation (9) represents a unified framework where both the model selection and the parameter estimation can be accomplished. In this Bayesian framework, Z and $p(\vartheta|\mathbf{D}, \mathbf{H}, I)$ represent the output for the Bayesian model selection and the output for the Bayesian parameter estimation, respectively.

4. Prior probability assignment

Prior to further analysis, both of the prior probabilities in Eq. (9) need to be assigned based on available information. Jaynes (1968) introduced a method encoding the known information into a prior probability assignment, which is referred to as the maximum entropy method (Xiang et al., 2022). Sections 4.1 and 4.2 demonstrate how the two prior probabilities are assigned based on the principle of maximum entropy.

4.1 Likelihood assignment

The likelihood is determined by the probabilities of the residual errors, which are the difference between the experimental data and the model with the parameter set at each datum in the frequency domain. The only information known prior to the analysis is that the residual errors possess a finite but unknown variance due to the fact that the multipole models are capable of describing the data well. Based on the principle of maximum entropy without any other information, the overall likelihood function is assigned to a product of all the error probabilities at each data point (Xiang, 2020),

$$p(\mathbf{D}|\vartheta, \mathbf{H}, I) = \frac{\Gamma(K/2)}{2} \left(\pi \sum_{k=1}^K \epsilon_k^2 \right)^{-K/2}, \tag{10}$$

with

$$\epsilon_k^2 = \text{Re}^2(\mathbf{D} - \mathbf{H}) + \text{Im}^2(\mathbf{D} - \mathbf{H}), \tag{11}$$

Table 1. Prior probability assignment for the four parameters.

$\Pi(G_\infty) = \text{uniform}(-1, 1)$	$\Pi(C_s) = \text{uniform}(-1000, 1000)$
$\Pi(A_q) = \text{uniform}(-40\,000, 40\,000)$	$\Pi(\alpha_s) = \text{uniform}(0, 20\,000)$
$\Pi(\lambda_q) = \text{uniform}(0, 75\,000)$	$\Pi(\beta_s) = \text{uniform}(-15\,000, 15\,000)$
$\Pi(B_s) = \text{uniform}(-10\,000, 10\,000)$	

where $\Gamma(\dots)$ is the standard gamma function, and ϵ_k is the residual error at a certain datum k . No more than the available information is encoded into this assignment of the likelihood function, and the likelihood assignment excludes bias for which there is no prior knowledge (Xiang, 2020).

4.2 Prior probability of model parameters

The analysis will not inject any preference for certain values of each individual parameter over the others. This is the only information that should be encoded in the Bayesian analysis when assigning the prior probability of the parameters encapsulated in the multipole model. The prior probability assignment applies again the principle of maximum entropy. Following the normalization constraint of a proper probability that has to be integrated to unity over the entire parameter space, the principle of maximum entropy assigns the prior probability uniformly distributed over a wide parameter range (Jaynes, 1968). The coefficients (model parameters) in Eq. (2) are assigned to the probability density functions as listed in Table 1.

5. Nested sampling

The Bayesian inference applied to the admittance estimation requires numerical evidence calculations. This work applies nested sampling proposed by Skilling (2006) to calculate the Bayesian evidence that is of central importance for the unified Bayesian framework.

Nested sampling is a Markov chain Monte Carlo method and is designed to thoroughly explore the entire parameter range. Here are the general main steps for the numerical implementation of nested sampling for every model (Fig. 1). First, an initial population of 500 samples with the uniform probability densities assigned to all the parameters as discussed previously in Sec. 4.2 is generated, and Eq. (10) evaluates the likelihood value of each sample within this population. This population remains alive during the whole iteration run. Then the parameter set associated with the lowest likelihood within this population is stored at the end of a separate sample list. For convenience, this sample that was stored into the sample list is denoted as “sample 1” in the following. For the next step, the perturbation of the parameters corresponding to sample 1 with parameters generated randomly over the parameter space will not stop until the likelihood value of the new sample is higher than sample 1. Once the likelihood of the new sample is higher, sample 1 is replaced with this new one in the initial population. After the initial population is updated (the number of the population is still 500), the new lowest likelihood value within the population is chosen for the next loop of recording and perturbing. With the samples being perturbed, again and again, the sample population would converge, or the sampling would stop when reaching a predefined maximum number of iterations. In this way, the sample list recording the likelihood values together with corresponding parameters is already sorted along a monotonically increasing sequence, and the summation of the likelihood sequence along an approximated shrinkage in the list approximates the evidence of the model (Skilling, 2006),

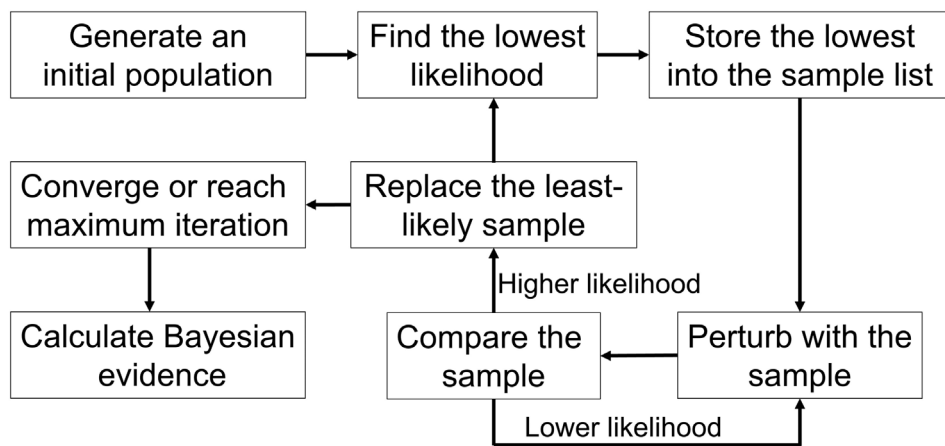


Fig. 1. General procedure for the practical implementation of nested sampling for each single model.

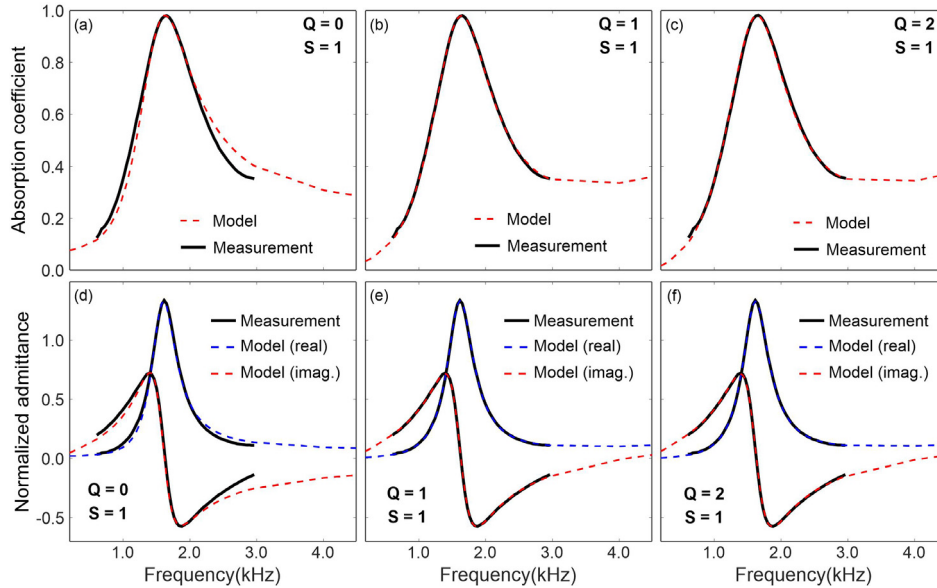


Fig. 2. Examples for absorption coefficients and surface admittance model sampling from the measured data with different orders of Q and S . Solid line, measured surface admittance; dashed lines, admittance models associated with parameters obtained from Bayesian sampling. Q is the number of real-valued poles, and S is the number of complex-valued poles.

which is used for ranking the models. Once the model is selected based on the Bayes factor in Eq. (6), the evidence value of the selected model is then used to evaluate the normalized posterior probability using the recorded list, which is already available upon the nested sampling. The posterior is the key quantity for estimating the mean and standard deviations of the model parameters. Two exploration criteria, maximum likelihood and the maximum number of iterations, are used as indicators for when the sampling should stop. If the logarithmic likelihood value in the sample list is higher than the predefined maximum likelihood 100 times (this constraint may vary for different data), the sampling is considered as converging. Or when the maximum number of iterations is met, the nested sampling will stop as well.

6. Experimental results

Figure 2 presents examples of the sampling results for three different admittance models. Note that the absorption coefficient in Fig. 2(a) is calculated from the surface admittance in Fig. 2(b). The material under test is glass beads of 2 mm in diameter that were deposited in a 45 mm diameter impedance tube in a random manner over 40 mm thickness (Horoshenkov et al., 2019).

Figure 3 illustrates the Bayes factors (as mentioned in Sec. 3.1) calculated from the evidence of the Bayesian inference for the models with different numbers of parameters. The Bayes factor is generally getting higher with the order of model getting higher. However, more computational effort is required by the more complicated models as well, since the increase in Q and S leads to more parameters in the estimation. More profoundly, the acoustic simulations require more computations for all the boundary elements assigned to this admittance. Undesirable inaccuracy and overfitting may

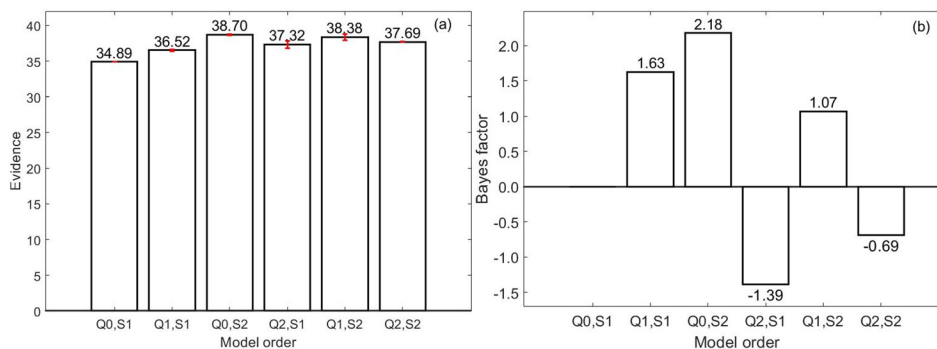


Fig. 3. Bayes evidence estimates. (a) Bayes evidence; (b) Bayes factors over the models with different number of poles. The Bayes's factors are the ratio of the evidence of the model over the model on its left side.

Table 2. Predicted parameters from Bayesian parameter estimation for a $\{Q = 1, S = 1\}$ broadband admittance model.

Parameter	Mean		Variance	Parameter	Mean		Variance
G_∞	0.469	\pm	0.013	C_1	-263	\pm	1.863
A_1	-26 062	\pm	529	α_1	1530	\pm	1.376
λ_1	55 250	\pm	588	β_1	10 063	\pm	1.274
B_1	2019	\pm	2.091				

occur when the model gets too complicated. As presented in Fig. 2, the data match to the model has a significant increase in accuracy when the multipole model is changed from Q0S1 to Q1S1. However, when the order of Q is increased to 2, the accuracy increase is insignificant. The Q2S1 model tends to fit the data well, including the noise. As demonstrated in Fig. 3(a), the Bayesian evidence goes down with the number of real poles Q shifted from 1 to 2, suggesting the Q2S1 is an overfitted model.

Given the data in this example, the Bayes factor of Q0S2 over Q1S1 model is the highest, suggesting that Q0S2 model is most preferred by the data over Q1S1 model. The Bayes factor of Q1S1 over Q0S1 model is also a positive, significant value. In Fig. 3(a), the evidence reaches the highest level with Q0S2 model. Both Q1S1 model and Q0S2 model are capable of fitting the data well, and they are the best choices based on Bayesian model selection. In consideration of the model complexity and accuracy associated with Q and S, the model with one real-valued pole and one pair of conjugate poles is sufficient to predict the desired surface admittance. Table 2 lists the estimated values of the model with Q1S1.

The boundary conditions in the real world, however, are more complex. They may not be as simple as the surface admittance presented in Fig. 2. Therefore, this work also tests performance of Bayesian inference when dealing with a more complex boundary with multi-layer micro-perforated panel absorbers (Xiang et al., 2022). Figure 4 presents an example of the Bayesian inference results for this complex boundary. Note that the numerical data of the boundary come from a recent design (Xiang et al., 2022). The three-layered micro-perforated panel absorber provides a high absorption coefficient of ≤ 0.8 between 350 and 2.5 kHz. The Bayesian model selection applied to the complex-valued surface admittance of the sound absorber prefers a multipole model of $Q = 1; S = 3$ as indicated by Fig. 4(c). More complicated models would also fit the data well but would be overly redundant.

In a similar fashion as in Fig. 3, Fig. 4(c) illustrates the Bayes factors and Bayesian evidence for the complex boundary. Among these six models, the Bayes factor of Q1S3 model over Q2S2 model is the highest, which means that data prefer the Q1S3 over Q2S2 the most. Note that any models with a lower number of complex pole pairs are unable to describe the designed multi-layer boundary well.

With the capability of fitting the measurement data and predicting the complex boundary conditions beyond the measurement range, multipole model-based Bayesian inference is well suited in estimating the arbitrary frequency-dependent boundary condition.

7. Concluding remarks

The present work applies the Bayesian method to wave-based broadband multipole models, evaluating them against measured frequency-dependent surface admittance of a porous material and a numerically designed arbitrary boundary. The higher level of inference, Bayesian model selection, estimates the orders of the multipole model, and the lower level of inference, Bayesian parameter estimation, estimates the parameter values of the model selected in the higher level. Employment of the nested sampling enables thorough exploration over the parametric space so as to be able to estimate the Bayesian evidence, being key quantities in the unified Bayesian framework. Therefore, both levels of Bayesian inference can be implemented within the unified Bayesian framework. Bayesian analysis provides a reliable method for the boundary

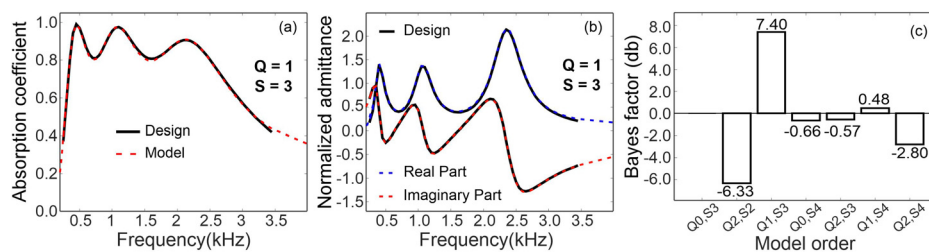


Fig. 4. An example of surface absorption and admittance coefficient along with the Bayes factor evaluations. (a) Absorption coefficient with Q1S3 model for the complex boundary; (b) surface admittance with Q1S3 model; (c) Bayes factors over the models with different numbers of poles for the complex boundary.

estimation problem and an acceptable approach to predict the frequency-dependent boundary based on frequency-dependent surface admittance from either experimental measurements or numerical designs. The current work has focused on the concise broadband model of the boundary given the surface impedance/admittance measurements. Further effort should be made to implement the wave-based room-acoustic simulations so as to verify and validate the broadband boundary model.

References and links

- Bin, J., Yousuff Hussaini, M., and Lee, S. (2009). "Broadband impedance boundary conditions for the simulation of sound propagation in the time domain," *J. Acoust. Soc. Am.* **125**(2), 664–675.
- de l'Epine, Y. B., Chazot, J.-D., and Ville, J.-M. (2005). "Bayesian identification of acoustic impedance in treated ducts," *J. Acoust. Soc. Am.* **138**(1), EL114–EL119.
- Dragna, D., Pineau, P., and Blanc-Benon, P. (2015). "A generalized recursive convolution method for time-domain propagation in porous media," *J. Acoust. Soc. Am.* **138**(2), 1030–1042.
- Fung, K.-Y., and Ju, H. (2001). "Broadband time-domain impedance models," *AIAA J.* **39**(8), 1449–1454.
- Horoshenkov, K. V., Hurrell, A., and Groby, J.-P. (2019). "A three-parameter analytical model for the acoustical properties of porous media," *J. Acoust. Soc. Am.* **145**(4), 2512–2517.
- Jaynes, E. T. (1968). "Prior probabilities," *IEEE Trans. Inf. Theory* **4**(3), 227–241.
- Kass, R. E., and Raftery, A. E. (1995). "Bayes factors," *J. Am. Statist. Assoc.* **90**(430), 773–795.
- Pind, F., Engsig-Karup, A. P., Jeong, C.-H., Hesthaven, J. S., Mejling, M. S., and Strømmand-Andersen, J. (2019). "Time domain room acoustic simulations using the spectral element method," *J. Acoust. Soc. Am.* **145**(6), 3299–3310.
- Pind, F., Jeong, C.-H., Engsig-Karup, A. P., Hesthaven, J. S., and Strømmand-Andersen, J. (2020). "Time-domain room acoustic simulations with extended-reacting porous absorbers using the discontinuous Galerkin method," *J. Acoust. Soc. Am.* **148**(5), 2851–2863.
- Reymen, Y., Baelmans, M., and Desmet, W. (2008). "Efficient implementation of Tam and Auriault's time-domain impedance boundary condition," *AIAA J.* **46**(9), 2368–2376.
- Rienstra, S. (2006). "Impedance models in time domain, including the extended Helmholtz resonator model," in *Proceedings of the 12th AIAA/CEAS Aeroacoustics Conference*, May 8–10, Cambridge, MA, paper 2006-2686.
- Skilling, J. (2006). "Nested sampling for general Bayesian computation," *Bayesian Anal.* **1**(4), 833–859.
- Troian, R., Dragna, D., Bailly, C., and Galland, M.-A. (2017). "Broadband liner impedance reduction for multimodal acoustic propagation in the presence of a mean flow," *J. Sound Vib.* **392**, 200–216.
- Xiang, N. (2020). "Model-based Bayesian analysis in acoustics—A tutorial," *J. Acoust. Soc. Am.* **148**(2), 1101–1120.
- Xiang, N., Fackler, C. J., Hao, Y., and Schmitt, A. A. J. (2022). "Bayesian design of broadband multilayered microperforated panel absorbers," *J. Acoust. Soc. Am.* **151**(5), 3091–3103.